https://doi.org/10.5194/hess-2021-310
Preprint. Discussion started: 11 June 2021
© Author(s) 2021. CC BY 4.0 License.

Hydrology and Earth System Sciences
Discussions

Development and parameter estimation of snowmelt models using spatial snow-cover observations from MODIS

Dhiraj Raj Gyawali and András Bárdossy
Institute for Modelling Hydraulic and Environmental Systems (IWS), University of Stuttgart
Correspondence: Dhiraj Raj Gyawali (dhiraj.gyawali@iws.uni-stuttgart.de)

Abstract. Given the importance of snow on different land and atmospheric processes, accurate representation of seasonal snow evolution including distribution and melt volume, is highly imperative to any water resources development trajectories. The limitation of reliable snow-melt estimation in these regions is however, further exacerbated with data scarcity. This study attempts to develop relatively simpler extended degree-day snow-models driven by freely available snow cover images in snow-dominated regions. This approach offers relative simplicity and plausible alternative to data intensive models as well as in-situ measurements and have a wide scale applicability, allowing immediate verification with point measurements.

The methodology employs readily available MODIS composite images to calibrate the snow-melt models on snow-distribution in contrast to the traditional snow-water equivalent based calibration. The spatial distribution of snow cover is simulated using different extended degree-day models calibrated against MODIS snow-cover images for cloud-free days or a set of images representing a period within the snow season. The study was carried out in Baden-Württemberg in Germany, and in Switzerland. The simulated snow cover show very good agreement with MODIS snow cover distribution and the calibrated parameters exhibit relative stability across the time domain.

The snow-melt from these calibrated models were further used as standalone inputs to a 'truncated' HBV without the snow component in Reuss (Switzerland), and Horb and Neckar (Baden-Wuerttemberg) catchments, to assess the performance of the melt outputs in comparison to a calibrated standard HBV model. The results show slight increase in overall NSE performance and a better NSE performance during the winter. Furthermore, 3-15% decrease in mean squared error was observed for the catchments in comparison to the results from standard HBV. The increased NSE performance, albeit less, can be attributed to the added reliability of snow-distribution coming from the MODIS calibrated outputs.

This paper highlights that the calibration using readily available images used in this method allows a flexible regional calibration of snow cover distribution in mountainous areas across a wide geographical extent with reasonably accurate precipitation and temperature data. Likewise, the study concludes that simpler specific alterations to processes contributing to snow-melt can contribute to identifying the snow-distribution and to some extent the flows in snow-dominated regimes.

1 Introduction

Reliable representations of spatial distribution of seasonal snow and subsequent snow-melt are critical challenges for hydrological estimations, given their crucial relevance in mountainous regimes especially because of the high sensitivity to climate

https://doi.org/10.5194/hess-2021-310
Preprint. Discussion started: 11 June 2021
© Author(s) 2021. CC BY 4.0 License.

Hydrology and Earth System Sciences
Discussions

change. Considering the snow effect on land and atmospheric processes, accurate representation of seasonal snow evolution is thus highly imperative to strengthen water resources development trajectories in these regions (Kirkham et al., 2019; Schmucki et al., 2014; He et al., 2014). Various modeling and measurement techniques are currently in practice which attempt to estimate this distribution of snow but these methods hold their own limitations. Prior studies on the comparison of snow models (Feng et al., 2008; Rutter et al., 2009) have highlighted the higher reliability of complex models in simulating the snow conditions. However, depending upon the complexities of the models, there exists big differences in model results. Relatively accurate physically based models are highly data intensive, which is mostly a big limitation in mountainous catchments around the world. Likewise, in-situ measurements of snow-depth providing accurate measures of snow depth can seldom cover a wider spatial extent and are prone to be non-representative due to local influences. Lack of snow-depth information and to some extent, persistent cloud cover in the mountains limit the standalone usage of Remote-sensing images in snow estimation (Tran et al., 2019). However, these images can provide a plausible alternative to ground based data especially in the data scarce mountain regions, since their resolution and availability do not depend on the mountainous terrain (Parajka and Blöschl, 2008).

The MODerate resolution Image Spectralradiometer (MODIS) (Hall et al., 2006) on board Terra and Aqua satellites are the one of the most extensively used snow cover products worldwide for snow cover monitoring owing to their daily temporal resolution and a high spatial resolution of 500m at the Equator. The cloud obstruction in MODIS, though significant, can be reduced combining the Aqua/ Terra MODIS images and other spatio-temporal filtering techniques (Tran et al., 2019; Gafurov and Bárdossy, 2009; Wang and Xie, 2009). Simple distributed snow-melt modeling approaches incorporating readily available meteorological data and these cloud filtered remote sensing images can be used to estimate the spatial extent that are free from highly localized influences. These simpler models offer a wide scale applicability and allow immediate verification with point measurements and this holds a high relevance in data scarce regions.

Against this backdrop, this work aims to implement a methodology using MODIS snow cover images to identify and to calibrate the melt models to estimate a time-continuous spatial snow extent in snow dominated regimes. Widely used and computationally simplistic temperature index models with low data requirement are considered in the study and are modified wherever possible, to gain enhanced model performance. Modifications to the models include a simple degree model followed by incorporation of different aspects governing snow hydrology such as precipitation induced melt, radiation, topography, and land use.

The main objective of this research is to develop a flexible snow-melt module useful for distributed hydrologic modeling, applicable in mountainous regimes across a wide geographical extent, with parameters which can be estimated by MODIS or other satellite-based snow cover products. Furthermore, calibration using readily available images proposed in this method, offers adequate flexibility and computational efficiency, albeit the simplicity, to calibrate melt models on an individual or a set of images and estimate the snow distribution in mountainous areas across different regions with reasonable precipitation and temperature data. This study intends to obtain a time continuous spatial snow cover and resulting melt which can be as a stand-alone input, coupled with distributed hydrological models to improve the model predictions.

https://doi.org/10.5194/hess-2021-310
Preprint. Discussion started: 11 June 2021
© Author(s) 2021. CC BY 4.0 License.

Hydrology and Earth System Sciences
Discussions
Open Access
EGU

2 Study Area

As explained above, this study attempts to test the efficacy of the aforementioned approach in the mountainous / snow dominated regimes. The study area is, thus selected as two distinct snow-regimes, a) characterized by intermittent snow and b) characterized by partly longer duration snow. For the former, Baden-Wuerttemberg region in Germany was selected. Whole of Switzerland was considered to represent the long duration snow for the study. Figure 1 below shows the study area:

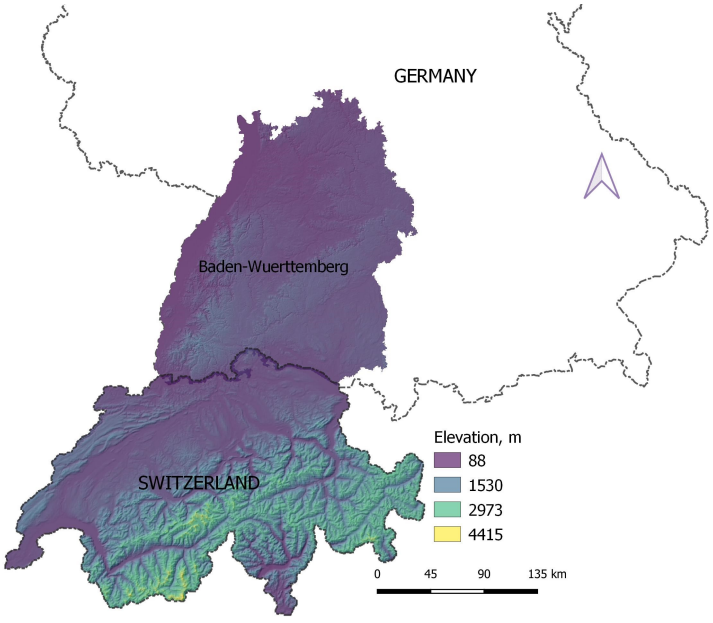

Figure 1. Map of the study area showing Baden-Wuerttemberg in Germany and Switzerland with elevation

The Baden-Wuerttemberg region includes the Schwabian Alps with the elevation rising to 1465 masl from a lowest of 88 masl. Likewise, Switzerland includes the Swiss Alps region which covers the perennial snow/glacier area. The elevation ranges from below 200 to 4415 masl. The study areas exhibit an average snow season from October to April in Germany and September to June in Switzerland.

3 Data and sources

The data used for the study are as briefly discussed as follows:

- **Hydro-meteorology** : Daily station meteorological data viz. precipitation, and minimum, maximum and mean temperatures from 2010-2018 were acquired for the study. For Germany, these variables were obtained from the Deutsche Wetterdienst (DWD), whereas for Switzerland the data was collected from Federal Office of Meteorology and Climatology (MeteoSwiss). Likewise daily discharge timeseries for selected catchments were collected to validate the efficacy

https://doi.org/10.5194/hess-2021-310
Preprint. Discussion started: 11 June 2021
© Author(s) 2021. CC BY 4.0 License.

Hydrology and Earth System Sciences
Discussions

of the approach in HBV model, from Bundesanstalt für Gewässerkunde (BFG) for Germany and Federal Office for the Environment (FOEN) for Switzerland.

- **Topography**: Shuttle Radiation Topography Mission (SRTM) 90m resolution Digital Elevation Model (DEM) was used in the study. The DEM was rescaled to match the MODIS resolution for consistency. Likewise, aspect and slope rasters were also obtained from this DEM.
- **Snow cover**: Daily MODIS Terra and Aqua Snow Cover products from 2010 to 2018 were used for calibrating the models and further analysis of snow distribution in the study regions. The resolution of the data is 500m at the Equator and 464m in the study region.

4 Data preparation

This study presents a distributed modeling approach with model computations done at pixel level of a gridded domain of 464m x 464m grids. For this, the input data were pre-processed and interpolated onto the aforementioned grid cellls. Following sequential steps were adopted for the data preparation.

4.1 Schema extraction

A gridded 464mx464m schema was extracted for both regions using the MODIS snow cover data as a reference. This schema was considered as the reference gridded domain for the data interpolation and model run.

4.2 MODIS pre-processing

The Aqua and Terra variants of MODIS snow cover data were downloaded and then pre-processed in different steps, viz. mosaicking, reprojection and clipping, using the GDAL module in Python. For uniformity, WGS84 UTM 32N was used as the base projection system.

4.3 Cloud removal

The pre-processed MODIS images were sequentially and spatio-temporally filtered using a cloud-removal procedure as described in Gafurov and Bárdossy (2009). The procedure follows the following steps:

(a) The first step checks the Aqua-Terra image combination. Pixels with clouds (255) in one of the images and land (0) or snow (1-100) in the other was replaced with the snow / land value and vice versa. The output is a combined raster with reduced cloud pixels. The combined raster was then reclassified as ‚0‘ and ‚1‘. No snow pixel values of the combined raster (0) are set to ‚0‘ and snow pixel values (1-100) are set to ‚1‘. Everything else is set to ‘No data’.

(b) The second step compares the preceding and succeeding days for a pixel under consideration. If both the days for the pixels are cloud-free with 0 or 1, the pixel under consideration will respectively get either 0 or 1 for the day.

https://doi.org/10.5194/hess-2021-310
Preprint. Discussion started: 11 June 2021
© Author(s) 2021. CC BY 4.0 License.

Hydrology and Earth System Sciences
Discussions
Open Access
EGU

(c) Likewise the third step compares two days backward and one day forward, and one day backward and two days forward combination to check for the cloud free days and infill accordingly, assuming consecutive snow or no-snow days.

(d) The fourth step compares the lowest elevation with snow and the highest elevation without snow for each day. Any pixel with elevation higher than the lowest elevation snow pixel would get ‚1' and the elevation lower than the highest elevation without snow would get ‚0'.

(e) The fifth step searches for '0' or '1' in a 8 pixel neighbourhood surrounding the cell. If the neighbourhood has a mode at least 4 valid values, the pixel will then be either '0' or '1'.

4.4 Spatial interpolation of precipitation and temperature

Both Baden-Wuerttemberg and Switzerland have a well distributed and dense network of meteorological stations. Figure 2 below shows the precipitation station network in Switzerland. The daily precipitation and temperature values from these stations were used for geostatistical interpolation onto the aforementioned schema for the regions. The Kriging process used are explained further in the following section.

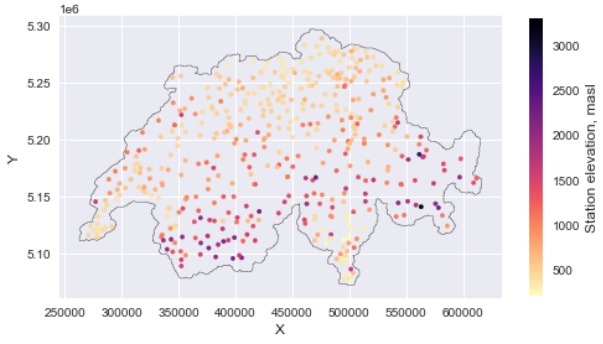

Figure 2. Precipitation station network in Switzerland

4.4.1 Daily temperature interpolation

For the interpolation of temperature data, External Drift Kriging (EKD) was opted in the regions under study, with station elevation as a drift. The station elevation exhibits strong correlation with the monthly and seasonal temperatures. Daily minimum, maximum and mean temperatures from 85 stations in Baden-Wuerrtemberg and 365 stations for Switzerland were used for the interpolation. Cross validation using leave-one-out approach was carried out to check for the applicability and the quality of the EKD interpolation.

https://doi.org/10.5194/hess-2021-310
Preprint. Discussion started: 11 June 2021
© Author(s) 2021. CC BY 4.0 License.

Hydrology and Earth System Sciences
Discussions

4.4.2 Daily precipitation interpolation

The daily precipitation sums were interpolated onto the schema using a detrended Residual Kriging (RK). To improve the precipitation interpolation in the higher elevation, a multiple linear regression (MLR) approach using directionally smoothed elevation was carried out for the study. Directional smoothing of elevation was done using half-space smoothing (Baŕdossy and Pegram, 2013). The approach uses a directionally transformed and smoothed topography to identify the effect of directional advection for each day. Eight different directions with 45 degrees incremental angles, and 3 different smoothing distances (2, 3 and 5 kms) were considered in this study. For each time-step, a simple optimization was done to assess the correlation of the precipitation with the shifted DEMs, and the best direction and the smoothing radius for the timestep were identified. This shifted and smoothed elevation was then used along with X and Y coordinates of the stations in the MLR to obtain precipitation estimates for stations. The residuals were then calculated for each day and ordinary Kriging was carried out to obtain the Kriged residuals. MLR estimated precipitation surfaces for each time step using X and Y coordinates and shifted elevation for the grid points were then added to the Kriged residual surfaces to obtain the final precipitation estimates. 224 stations in BW, and 449 stations in Switzerland were used in this study. Leave-one-out cross validation for each station was done and the rainfall and temperature Kriging performance was evaluated using Nash-Sutcliffe Efficiency (NSE, Eq. (1)) for each station.

$$NSE = 1 - \frac{\sum_{t=1}^{T} \left(Y_o^t - Y_m^t \right)^2}{\sum_{t=1}^{T} \left(Y_o^t - \bar{Y}_o^T \right)^2} \quad (1)$$

Where,

Y_m^t = Simulated ('Kriged') variable at time t,

Y_o^t = Observed variable at time t,

$\bar{Y}_o^T$ = mean of observed variable for the time period T,

T = length of timeseries,

5 Methodological Framework

The methodological framework applied for the study is shown below in Fig. 3 and is further discussed in subsequent sections.

6 Snow melt models

This study employs empirical, temperature-index melt modelling approach using the degree day factors. The degree day models are widely used owing to relatively easier interpolation of air temperature, and reasonable computational simplicity (Hock, 2003). This degree-day approach assumes melt rate as a linear function of the air temperature. Due to inherent large-scale

https://doi.org/10.5194/hess-2021-310
Preprint. Discussion started: 11 June 2021
© Author(s) 2021. CC BY 4.0 License.

Hydrology and Earth System Sciences
Discussions
Open Access
EGU

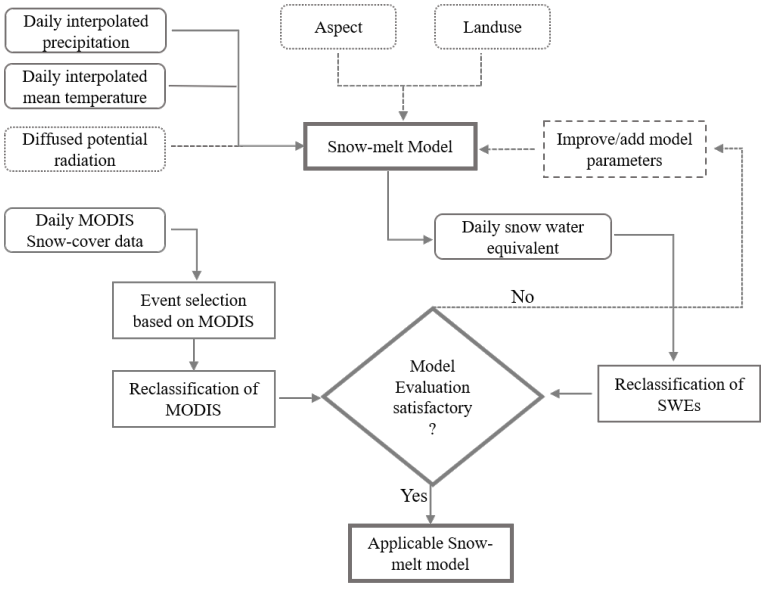

Figure 3. Methodological approach for the study

spatial variability in the mountain regions, distributed meteorological inputs, were employed to drive the different variants of the extended degree-day snow melt models on a daily timescale. The major parameters used in the models are defined below.

Where,

$P(t,x)$= precipitation amount at location x at time t, mm

$S(t,x)$= snow water equivalent amount at location x at time t, mm

$T_{av}(t,x)$= mean temperature at location x at time t, °C

$P_s(t,x)$ = water equivalent of precipitation falling as snow at location x at time t, mm

$M_s(t,x)$ = melt water amount at location x at time t, mm

T_T = threshold critical temperature defining snow or no snow, °C

D_s = dry degree day factor, $mm°C^{-1}$

$T_{mx}(t,x)$= maxmimum temperature at location x at time t, °C

$T_{mn}(t,x)$= minimum temperature at location x at time t, °C

The following model variants were used to estimate the snow-water equivalent (SWE, mm) and the resulting snow cover in each pixel. Different nomenclatures are given to the models for the ease of understanding. Each successive model represents a gradual parameter wise modification to the basic degree-day model.

6.1 Basic Degree-day Model (Model 1)

This model estimates the melt for each time-step as a linear function of the difference between daily mean temperatures and a threshold temperature value demarcating liquid precipitation and snow precipitation. A degree day factor controls the rate

https://doi.org/10.5194/hess-2021-310
Preprint. Discussion started: 11 June 2021
© Author(s) 2021. CC BY 4.0 License.

Hydrology and Earth System Sciences
Discussions
Open Access
EGU

of melt. Equation (2) calculates the amount of SWE available in pixel 'x' at time 't'. Similarly the snow-precipitation and the resulting melt are calculated with Eq.(3) as the model basis for each pixel, 'x' in the study domain.

$$S(t,x) = S(t-1,x) + P_s(t,x) - M_s(t,x), \tag{2}$$

Where,

$$P_s(t,x) = \begin{cases} P(t,x) & \text{if} \quad T_{av}(t,x) < T_T \\ 0 & \text{if} \quad T_{av}(t,x) \geq T_T \end{cases} \tag{3a}$$

$$M_s(t,x) = \begin{cases} 0 & \text{if} \quad T_{av}(t,x) < T_T \\ min(S(t,x), \quad D_s\ (T_{av}(t,x) - T_T) & \text{if} \quad T_{av}(t,x) \geq T_T \end{cases} \tag{3b}$$

6.2 Wet Degree-day Model (Model 2)

In addition to the temperature induced melt, this variant adds melt due to liquid water falling on the snowpack. This melt factor, henceforth referred to as D_w increases the melt from Eq.(3b) on days with precipitation higher than a threshold value. For a given wet day i.e., $P(t,x) > P_T$, the melt is calculated as in Eq.(4). For a dry day, melt is calculated as Eq.(3b).

$$M_s(t,x) = \begin{cases} 0 & \text{if} \quad T_{av}(t,x) < T_T \\ min(S(t,x), \quad D(t,x)\ (T_{av}(t,x) - T_T) & \text{if} \quad T_{av}(t,x) \geq T_T \end{cases} \tag{4}$$

Where,

$D(t,x)$ = D_s + D_w($P(t,x)$ - P_T)

P_T = Threshold precipitation depth beyond which the liquid precipitation contributes to melt, mm

D_w = the wet melt factor, $mm.mm°C^{-1}$

$D(t,x)$ = combined melt factor on wet days, $mm°C^{-1}$

https://doi.org/10.5194/hess-2021-310
Preprint. Discussion started: 11 June 2021
© Author(s) 2021. CC BY 4.0 License.

Hydrology and Earth System Sciences
Discussions
Open Access
EGU

6.3 Wet Degree-day Model with snowfall and snowmelt temperatures (Model 3)

This model includes different snowfall and snowmelt temperatures in Model 2 for a more accurate representation of the snowfall / -melt process. For temperatures in between, snow is linearly interpolated for the day as a proportion of the precipitation. The formulation of the model are given by Eqs.(5) and (6).

$$P_s(t,x) = \begin{cases} P(t,x) & \text{if} \quad T_{av}(t,x) < T_S \\ P(t,x) \cdot \left(\frac{T_{av}(t,x) - T_M}{T_S - T_{av}(t,x)} \right) & \text{if} \quad T_S \leq T_{av}(t,x) \leq T_M \\ 0 & \text{if} \quad T_{av}(t,x) > T_M \end{cases} \tag{5}$$

$$M_s(t,x) = \begin{cases} 0 & \text{if} \quad T_{av}(t,x) < T_M \\ min(S(t,x), \quad D(t,x) \ (T_{av}(t,x) - T_M)) & \text{if} \quad T_{av}(t,x) \geq T_M \end{cases} \tag{6}$$

Where,

T_S and T_M are the snowfall and snowmelt temperatures respectively.

6.4 Aspect distributed snowfall temperatures (Model 4)

This variant distributes the snowfall temperature in Model 3, according to the topographical aspect. The snowfall temperature distribution is done by Eq.(7) below:

$$T_{S,x} = T_{Smin} + (T_{Smax} - T_{Smin}) * [0.5 * \cos(aspect_x) + 1]^{PF} \tag{7}$$

Where,

T_{Smin} = lower bound of the snowfall temperature

T_{Smax} = upper bound of the snowfall temperature

$aspect_x$ = topographical aspect of grid 'x', (radians)

PF = power factor to distribute the aspect

6.5 Aspect distributed snowmelt temperatures (Model 5)

This model distributes the snowmelt temperature in Model 3 within a range defined by minimum and maximum snowfall temperature, according to the topographical aspect. The snowmelt distribution is represented by Eq.(8) below:

$$T_{M,x} = T_{Mmin} + (T_{Mmax} - T_{Mmin}) * [0.5 * \cos(aspect_x) + 1]^{PF} \tag{8}$$

https://doi.org/10.5194/hess-2021-310
Preprint. Discussion started: 11 June 2021
© Author(s) 2021. CC BY 4.0 License.

Hydrology and Earth System Sciences
Discussions

Where,

T_{Mmin} = lower bound of the snowfall temperature

T_{Mmax} = upper bound of the snowfall temperature

$aspect_x$ = topographical aspect of grid 'x', (radians)

PF = power factor to distribute the aspect

6.6 Radiation Induced melt Model (Model 6)

This model adds radiation induced melt to Model 5 by incorporating the diffused incident radiation on the snow pixel on a cloud-free day. The incident global radiation is calculated using a viewshed based algorithm "r.sun algorithm" (Hofierka and Suri, 2002; Neteler and Mitasova, 2002) and has an added advantage of radiation distribution in the valleys. Daily temperature difference (tmax -tmin) for each grids was also calculated using interpolated daily minimum and maximum temperatures and was used as a cloud cover proxy. For this study, pixels with a daily temperature difference above a certain threshold were assumed to be cloud free and this is where radiation induced melt became active. Likewise, temperature differences lesser than the threshold render the pixels cloudy. The diffusion factor ranging from 0.2 for clear sky conditions to 0.8 for overcast conditions diffuses the incoming radiation. The radiation induced melt is added to the melt outputs from the preceding models on cloudlfree pixels and is calculated using Eq.(9). Figure 4 below shows an example of diffused radiation calculated for a cloud free day in BadenWuerrtemberg.

$$M_{s-R}(t,x) = \begin{cases} (1-alb)\cdot r_{ind}\cdot R_D(t,x) & \text{if} \quad T_{mx}(t,x) - T_{mn}(t,x) \geq 5°\text{C} \\ 0 & \text{if} \quad T_{mx}(t,x) - T_{mn}(t,x) < 5°\text{C} \end{cases} \tag{9}$$

Where,

$M_{s-R}(t,x)$ = Radiation induced melt at grid x at time t, mm

$R_D(t,x)$ = Diffused radiation at gird x at time t, $Wh \cdot m^{-2} day^{-1}$

alb = Albedo of snow

r_{ind} = Radiation melt factor, $mm \cdot (Wh.m^{-2} day^{-1})$

$(T_{mx}(t,x) - T_{mn}(t,x))$ = temperature difference at time t, as a cloud proxy to define clear-sky and overcast conditions

6.7 Data requirement of the models

Table 1 below summarizes the input data requirement for each model indicating both spatial and temporal resolution. In addition to the data presented in the table, the daily MODIS snow-cover distribution is also required for model calibration and evaluation. Likewise, daily observed stream-flows are also required for calibration and validation of the HBV model.

https://doi.org/10.5194/hess-2021-310
Preprint. Discussion started: 11 June 2021
© Author(s) 2021. CC BY 4.0 License.

Hydrology and Earth System Sciences
Discussions

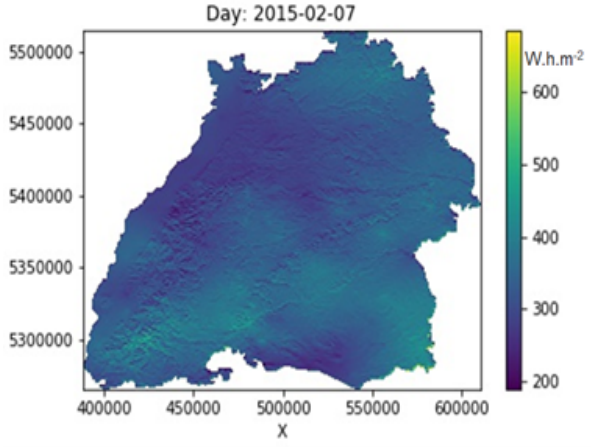

Figure 4. Illustration of diffused radiation calculated using r.sun.daily algorithm for Baden-Wuerttemberg

Table 1. Inputs required for the different model variants

Models	Spatial Inputs, (464 x 464m)		Spatiotemporal Inputs, (464 x 464m, daily)				
	DEM	**Aspect**	**PCP, mm**	**Mean temp., °C**	**Max./Min. temp, °C**	**Diffused Radiation,** $Wh.m^{-2}.day^{-1}$	**Cloud Info***
Model 1	yes	–	yes	yes	–	–	–
Model 2	yes	–	yes	yes	–	–	–
Model 3	yes	–	yes	yes	–	–	–
Model 4	yes	yes	yes	yes	–	–	–
Model 5	yes	yes	yes	yes	–	–	–
Model 6	yes	yes	yes	yes	yes	yes	yes

7 Model Reclassification

The snow-water equivalent (SWE, mm) obtained from the snow-models at each pixel were reclassified as '1' (snow) or '0' (no snow), thus simulating a snow-distribution pattern for the reference calibration event/duration. The reclassification was done based on a threshold level of 0.5mm (assuming a snowpack density of 20% ca.2.5mm of snow depth). The threshold depth was defined to ignore the transient snowfall events. Pixels with model-simulated SWE values greater than 0.5mm were considered as snowy pixels and values less than the threshold were considered pixels with no snow. Likewise, the MODIS images were also reclassified based on the snow proportion at each pixels. The pixel values from more than 0 to 100 were reclassified as '1' and the pixel values with'0' remain '0'. The rest of the values were reclassified as 'No Data' pixels and were not considered

https://doi.org/10.5194/hess-2021-310
Preprint. Discussion started: 11 June 2021
© Author(s) 2021. CC BY 4.0 License.

Hydrology and Earth System Sciences
Discussions

during the calibration. The reclassified MODIS image or a set of images with binary (0 or 1) values for a relatively cloud-free event or a duration during the winter was selected as the observed snow cover distribution for calibrating the models.

8 Model setup

8.1 Model calibration

The study employed a unique image-based pattern calibration approach in contrast to the more widely used calibration approaches using SWEs. As described in the previous section, the different extended degree-day models were calibrated on the reclassified MODIS-inferred snow cover distribution for a certain cloud-free day or for a duration within the snow season (eg. November-December) of a given year as observed reference. The major advantage of using image based calibration is the flexibility it offers to regionally calibrate the models on a single image for a certain cloud-free day, or on a set of images for a melt, onset season or even the whole time-series.

The calibration used a simple Brier score (BS) as the objective function (Eq.(10)). The BS is a score function that measures the accuracy of probabilistic predictions. It can also be inferred as the mean squared error as applied to these predicted probabilities. The BS in this study refers to the mean squared error between observed binary patterns of snow/no snow from MODIS and the ones simulated by the extended degree-day models. The Brier score varies between 0 and 1 with the values closer to ‚0' indicating better agreement between the model outputs and the MODIS image. Once the parameters were estimated for the model, it was then validated for cloud free days in different years and seasons. This was repeated for different variants of snow models described in the above sections.

$$BS = \frac{1}{N}\sum_{t=1}^{N}(f_t - O_t)^2 \tag{10}$$

Where,

f_t = simulated values, o_t = observed values

The Differential Evolution (DE) optimization scheme was considered in this study for the calibration process. The DE approach optimizes by iteratively trying to improve a candidate solution with regard to a given measure of quality. It provides a true global minimum of a multi modal search space regardless of the initial parameter values, allows faster convergence employing few control parameters and provides a single model parameter vector which is imperative to this study. The model parameters were estimated for each region assuming spatio-temporally constant/variable (wherever possible) parameter sets. Depending upon the model variants, some parameters were distributed based on aspect and elevation. The parameters were estimated within a plausible range as described in different snow modelling studies.

8.2 Model validation

The calibrated parameter sets were used to validate the simulated snow-patterns for different seasons in the same year and as well as other years. The validation was done on several individual images representing unique events, as well as on sets

https://doi.org/10.5194/hess-2021-310
Preprint. Discussion started: 11 June 2021
© Author(s) 2021. CC BY 4.0 License.

Hydrology and Earth System Sciences
Discussions

of images representing different seasons. Once the model performance was adequately validated and the parameters were deemed 'applicable', the models were run again to obtain the gridded melt outputs, assuming the model predicted both the snow distribution as well as the water content adequately. The melt outputs were then further validated using the modified version of the hydrological model Hydrologiska Byråns Vattenbalansavdelning (HBV) (Bergström, 1995), HBV. The HBV model was modified to have only the ‚liquid' component, thus omitting the snow process, and is henceforth termed as ‚Liquid HBV'. The melt outputs from the model variants were fed into the Liquid HBV as standalone inputs to evaluate the efficacy of the snow-melt models and subsequently the model performance in terms of overall hydrological response. The standard HBV model was calibrated against the observed flows and the performance of this HBV model was compared with the performance of the Liquid HBV with external melt. This process was repeated in different snow-fed catchments in Baden-Wuerttemberg (Neckar and Horb) and Switzerland (Reuss). Nash-Sutcliffe Efficiency (NSE, Eq.(1)) for overall, winter and snow days time-series was used to evaluate the performance of the melt inputs, where the simulated and observed variables refer to modelled and observed discharge at time 't'.

9 Results

9.1 Kriging Results

Residual Kriging incorporating X,Y coordinates and directionally smoothed DEMs was used for residual Kriging in Switzerland. Leave-one-out cross validation using Nash-Sutcliffe efficiency for the snow season (October – April) as evaluation function was done for 449 precipitation stations in Switzerland and 128 stations in Baden-Wuerttemberg. Table 2 below summarizes the mean Kriging performance across all the stations for both regions. The results suggest that the adopted Kriging procedure adequately mimics the daily precipitation from the stations in both regions. The NSEs range from 0.56 to 0.97 for the time period between 2010 and 2018 in Switzerland whereas for Baden-Wuerttemberg the values ranged from 0.72 to 0.97. The station locations along with the corresponding NSE performance in the Swiss region is shown in Figs. 5a and 5b below. The figures show that the NSE performance for the winter precipitation decreases with increasing elevation. This loss in performance can be attributed to less density of stations in the higher elevation. However, the NSE values of greater than 0.6 for all but one station indicate that the Kriging process works satisfactorily in the region. The precipitation Kriging in Baden -Wuerttemberg, however, did not depict a topographical trend in NSE performance, but the results highlight the applicability of the Kriging in the region. It can also be observed from Table 2 that the EKD Kriging was very much efficient in interpolating mean temperature in both the regions.

9.2 Model Results

9.2.1 Switzerland

For Switzerland, a relatively cloud-free MODIS image for 18th January 2012 was selected as a reference day with snow, and all the model variants were calibrated using this image. All of the six models reported good Brier scores. The normalized

https://doi.org/10.5194/hess-2021-310
Preprint. Discussion started: 11 June 2021
© Author(s) 2021. CC BY 4.0 License.

Hydrology and Earth System Sciences
Discussions
Open Access
EGU

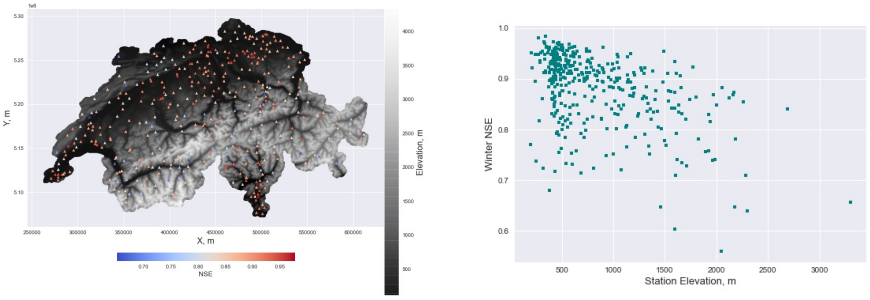

(a) NSE in different precipitation stations

(b) NSE performance of Kriged precipitation at different station elevation

Figure 5. Kriging performance in terms of NSE in Switzerland

Table 2. Summary of mean Kriging performance in the study regions

Region	Variables	Reference period	Pearson correlation	Rank correlation	RMSE	NSE	No. of stations
Switzerland	Mean temp.	Overall	0.99	0.99	1.13	0.971	365
		Winter	0.978	0.977	1.288	0.936	
	Precipitation	Overall	0.933	0.83	2.637	0.856	449
		Winter	0.95	0.823	2.166	0.883	
Baden-Wuerttemberg	Mean temp.	Overall	0.992	0.992	0.938	0.978	85
		Winter	0.979	0.976	0.982	0.943	
	Precipitation	Overall	0.907	0.876	2.295	0.811	128
		Winter	0.96	0.912	1.479	0.901	

confusion matrices calculated for the reference day with all models along with their Brier scores are shown in Fig. 6a. The top-left, top-right, bottom-right and bottom-left boxes of a confusion matrix plot respectively indicate the proportions of true negatives (both 'no snow'), false positives (MODIS: 'no snow', simulated: 'snow'), true positives (both 'snow') and false negatives (MODIS: 'snow', simulated: 'no snow'). These result plots show gradual improvement in the model performance with additional parameters, with the Brier scores ranging from 0.044 to 0.0365. Model 6 including the radiation induced snowmelt shows the best performance among the models, with a Brier score value of 0.0365. Model 5 has the next closest match. The models 5 and 6 both improve the true negatives and true positives with Model 6 exhibiting lesser false recognition of snow. With a more balanced representation of false and true positives and negatives, Model 6 was selected as the best model and is thus used as the reference model for further analysis. Figure 6b shows the simulated snow image for the reference day using

https://doi.org/10.5194/hess-2021-310
Preprint. Discussion started: 11 June 2021
© Author(s) 2021. CC BY 4.0 License.

Hydrology and Earth System Sciences
Discussions

the best model along with the differences from MODIS. The left plot in the figure is the MODIS image for the reference day, the central plot shows the simulated image for the day and the right one shows the differences in prediction.

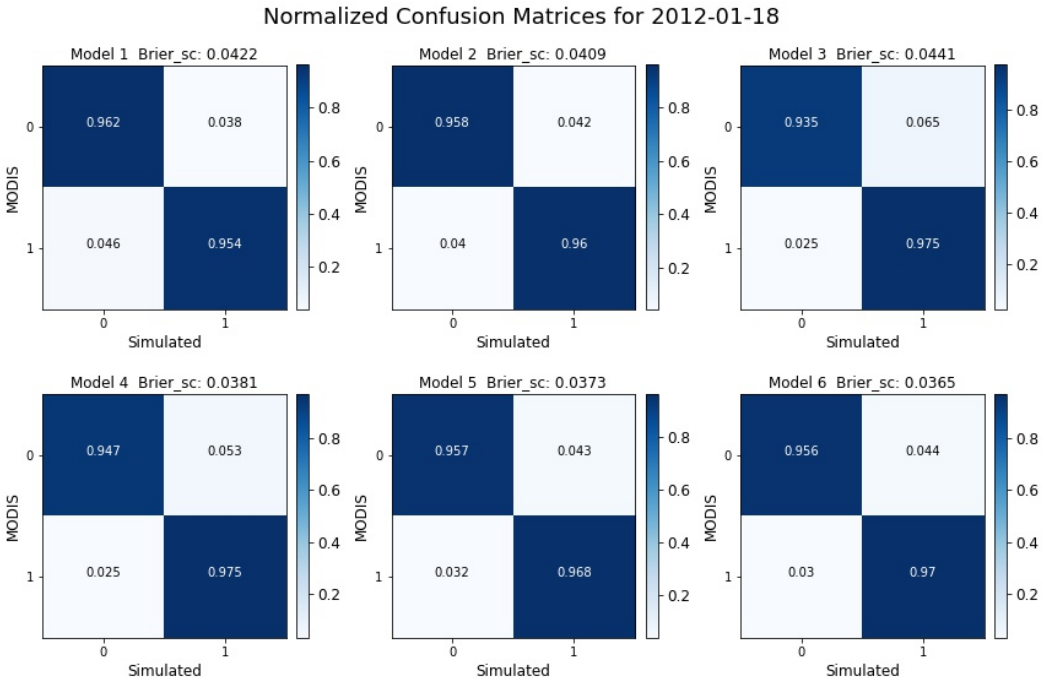

(a) Normalized Confusion matrices from all models for the reference day (‚1': Snow, ‚0': No snow)

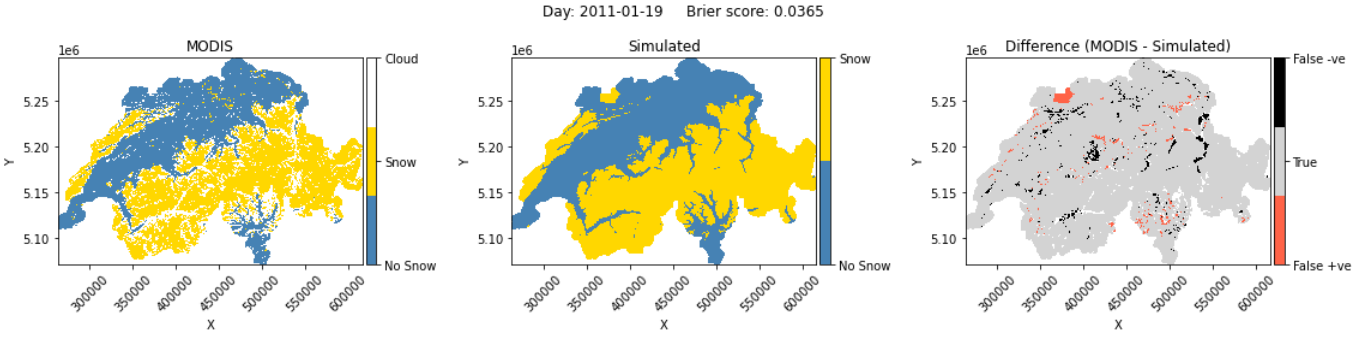

(b) MODIS inferred snow distribution (left) vs Model 6 simulated distribution (centre) and differences between MODIS and simulated (right)

Figure 6. Simulation results for the reference day of 2012-01-18 for Switzerland

Figure 7 below shows the normalized confusion matrix of MODIS snow-cover and snow-cover simulated by the best model (driven by the parameters calibrated for the aforementioned reference day), for a period of 2011-01-01 to 2018-12-31. The

https://doi.org/10.5194/hess-2021-310
Preprint. Discussion started: 11 June 2021
© Author(s) 2021. CC BY 4.0 License.

Hydrology and Earth System Sciences
Discussions

matrix reflects very good capability of the model to identify and predict snow (‚1') with 0.947 and no-snow pixels (‚0') with 0.932 as a proportion of all the valid pixels. The false negatives and true negatives amount to less than 10 % of the total pixels.

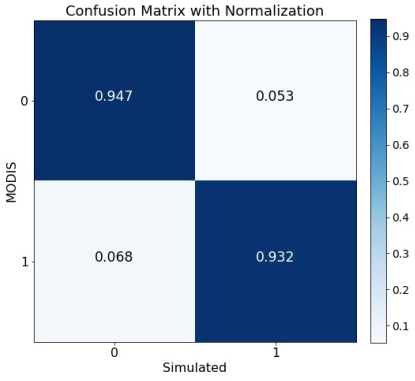

Figure 7. Normalized confusion matrix of the simulation results for 2011-01-01 to 2018-12-31 for Switzerland

9.2.2 Baden-Wuerttemberg

The different snow models were also tested in Baden-Wuerttemberg region in Germany. The region was selected to test the efficacy of the approach in shorter duration snow region. MODIS image for the day 2010-02-27 was selected as the reference image for calibration. All the models were able to mimic the snow-distribution pattern for the reference day. Model 6 performed the best in terms of the Brier score and is shown in Fig. 8. The models were then validated for different cloud free days in different years.

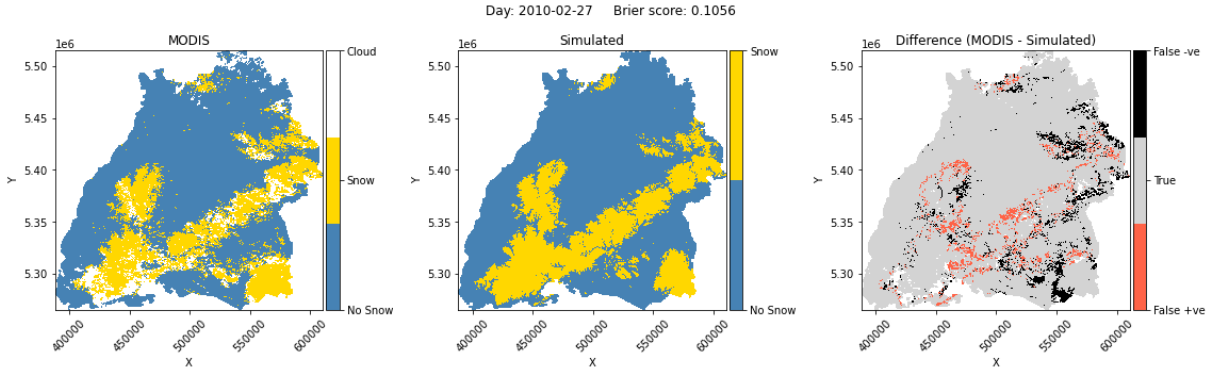

Figure 8. MODIS inferred snow distribution (left) vs Model 6 simulated distribution (centre) and differences between MODIS and simulated (right)

https://doi.org/10.5194/hess-2021-310
Preprint. Discussion started: 11 June 2021
© Author(s) 2021. CC BY 4.0 License.

The models were able to capture the snow-distribution reasonably well in Baden-Wuerttemberg, albeit not as good as in Switzerland. Short duration snow or lesser snow availability can be attributed to this drop in model performance, as it imparts added uncertainty in model prediction. Based on the Brier scores on the validation days, Model 6 was selected as the reference model and hereon used for further analysis based on the validation data. Figure 9 shows the normalized confusion matrix based on Model 6 simulation from 2011-01-01 till 2015-12-31. It is evident from the figure that the model is able to simulate the snow-distribution well enough with 83 % of correctly identified 'snow' pixels. This performance, however, shows that the model still has room for improvement especially in regions like Baden-Wuerttemberg, where snow-melt is a major source of water.

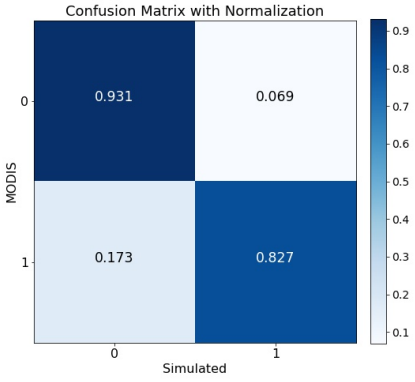

Figure 9. Normalized confusion matrix of the simulation results for 20110101 to 20151231

9.2.3 Transferability of model parameters

To test for the transferability of the model parameters through different seasons, the calibrated model parameters were also validated for the onset and melting seasons of different years. The goal here, was to obtain a relatively stable parameter-set across the time domain that can depict comparable model performance for different seasons. The best model (Model 6) is used as the reference model in this analysis. Snow onset periods (Oct-Dec for Switzerland and Nov-Dec for Baden-Wuerttembeg) and melting periods (Jan-Mar for Switzerland and Jan-Feb for Baden-Wuerttemberg) for 2010 - 2015 were selected as the calibration and validation periods. The models were calibrated for onset periods for each year and then run to forecast the snow distribution in the corresponding melting season as well as to hindcast the snow distribution in the onset and melting seasons of preceeding year. Tables 3 and 4 below summarize the model performance (Brier score) for different hindcast and forecast periods for Switzerland and Baden-Wuerttemberg, respectively. The orange, green and yellow highlights depict hindcast, calibration and forecast for each year.

As an illustration, in Switzerland, the model was calibrated for 2011 Oct-Dec period and used to hindcast the snow cover distribution in the preceding onset (2010 Oct-Dec) and melt (2011 Jan-Mar) seasons, and forecast for the corresponding melting

https://doi.org/10.5194/hess-2021-310
Preprint. Discussion started: 11 June 2021
© Author(s) 2021. CC BY 4.0 License.

Hydrology and Earth System Sciences
Discussions

Table 3. Model calibration, hindcast and forecast performance in different seasons for Switzerland

Validation Periods	Calibration period						
	2010/ Oct-Dec	2011/ Oct-Dec	2012/ Oct-Dec	2013/ Oct-Dec	2014/ Oct-Dec	2015/ Oct-Dec	Jan 18 2012
2010/ Jan-Mar	0.06833						
2010/ Oct-Dec	0.06757	0.06849					0.07335
2011/ Jan-Mar	0.06067	0.06609					
2011/ Oct-Dec		0.08531	0.0862				0.09061
2012/ Jan-Mar		0.05118	0.05966				
2012/ Oct-Dec			0.08035	0.08548			0.08855
2013/ Jan-Mar			0.06648	0.0567			
2013/ Oct-Dec				0.10058	0.12441		0.10636
2014/ Jan-Mar				0.05104	0.06307		
2014/ Oct-Dec					0.07281	0.07484	0.0894
2015/ Jan-Mar					0.09987	0.08274	
2015/ Oct-Dec						0.09097	0.09746
2016/ Jan-Mar						0.09371	
	Hindcast	Calibration	Forecast				

Table 4. Model calibration, hindcast and forecast performance in different seasons for Baden-Wuerttemberg

Validation Periods	Calibration period							Swiss Parameters for Jan 18, 2012
	2010/ Nov-Dec	2011/ Nov-Dec	2012/ Nov-Dec	2013/ Nov-Dec	2014/ Nov-Dec	2015/ Nov-Dec	Feb 27 2010	
2010/ Jan-Feb	0.1191						0.1147	
2010/ Nov-Dec	0.0777	0.0853					0.0851	**0.083**
2011/ Jan-Feb	0.1790	0.2314					0.1854	
2011/ Nov-Dec		0.2398	0.2383				0.2553	**0.255**
2012/ Jan-Feb		0.2982	0.2805				0.2763	
2012/ Nov-Dec			0.2342	0.2365			0.2411	**0.24**
2013/ Jan-Feb			0.2153	0.1794			0.1707	
2013/ Nov-Dec				0.2963	0.373		0.3239	**0.324**
2014/ Jan-Feb				0.2185	0.3059		0.2394	
2014/ Nov-Dec					0.228	0.2344	0.2356	**0.236**
2015/ Jan-Feb					0.2449	0.2506	0.1305	
2015/ Nov-Dec						0.2045	0.209	
	Hindcast	Calibration	Forecast					

season (2012 Jan-Mar). The 2011 model performance was then compared with the hindcast of the succeeding calibration and the forecast of the previous calibration. Here in this example the hindcast performance (0.068 for Oct-Dec 2010 and 0.0661 for Jan-Mar 2011) is very close to the ones simulated by the 2010 model (0.0675 for calibration period and 0.061 for forecast period). The other results are also comparable throughout the years. These results are again compared with the model calibrated on a single day image in the last column (2012-01-18) described in earlier sections. Here as well, the model calibrated on a single image is able to adeptly track the distribution in different snow-onset and melt seasons in different years, without much loss in performance. The calibrated parameters for the aforementioned seasons and the reference day are shown below in Tables 5a and 5b. The P_T and D_w parameters are less sensitive and the fluctuations in these parameters do not have major implications on the model performance. Apart from these parameters, it is apparent that the individual parameter values do not fluctuate a

https://doi.org/10.5194/hess-2021-310
Preprint. Discussion started: 11 June 2021
© Author(s) 2021. CC BY 4.0 License.

Hydrology and Earth System Sciences
Discussions
Open Access
EGU

lot and are more or less stable in Switzerland. The calibrated parameters from the single day calibration, understandably shows quicker melt with low values of snowmelt temperatures, apart from which the parameter sets can be inferred as temporally stable for the said periods for this region. However, individual parameter values here have a wider spread in BW for the same periods in comparison with Switzerland. As discussed above, this can be attributed more to the lesser and more uncertain availability snow in different seasons. This shows that with continuous updating of the model for each season, the model can forecast the snow-availability.

Table 5. Calibrated parameter sets for Oct-Dec periods in different years

(a) Switzerland

	D_s	P_T	D_w	T_s	T_{Mmin}	T_{Mmax}	PF	r_{ind}	alb
2010	1.6412	6.677	0.2098	-1.787	0.673	1.228	1.0246	0.0021	0.77
2011	1.7396	7.8749	0.1358	-2.7674	1.325	1.8507	3.6165	0.0027	0.6242
2012	1.5386	0.5994	0.3021	-2.8419	1.4176	2.085	3.6551	0.006	0.8971
2013	1.5463	8.5786	0.6704	-2.5345	0.4018	0.6695	0.0899	0.006	0.8966
2014	1.5135	3.7622	0.0235	-2.9109	1.7374	2.2875	2.5869	0.0071	0.6862
2015	1.514	6.055	0.0493	-2.77	0.563	2.207	2.219	0.0035	0.8203
18-Jan-12	1.5935	8.1543	0.0002	-2.9109	-0.0867	0.2738	0.1177	0.004	0.78

(b) BadenWuerttemberg

	D_s	P_T	D_w	T_s	T_{Mmin}	T_{Mmax}	PF	r_{ind}	alb
2010	1.893	7.231	0.052	-2.853	1.032	1.108	4.5	0.009	0.817
2011	1.949	2.32	0.072	1.342	1.854	2.444	0.18	0.38	0.713
2012	2.64	6.204	0.066	1.214	1.992	2.148	1.366	0.2	0.8
2013	1.673	7.903	0.085	0.574	0.623	0.743	6.691	0.013	0.687
2014	2.664	9.01	0.466	-0.286	1.526	2.957	0.015	0.109	0.249
2015	1.587	3.074	0.003	-0.323	1.493	2.109	5.975	0.001	0.401
27-Feb-10	1.505	9.596	0.085	-2.891	0.239	0.359	0.731	0.01	0.788

9.2.4 Validation in Hydrological Models

Once the simulated snow cover distribution from the melt models were validated for cloud free days in the respective regions, the melt outputs from the models were used as standalone inputs to a modified HBV („the Liquid HBV“) and the resulting flows compared with the basic HBV model for the entire, winter and snow-days time-series. This was done for Neckar and Horb catchments in Baden-Wuerrtemberg and Reuss catchment in Switzerland. Horb, a tributary of the Neckar catchment, was selected as the catchment is predominantly snow-fed and shows direct response to snow-melt. The basic HBV model was first calibrated for each of the catchments and the calibrated parameters (without the snow parameters) were used in the liquid HBV model and the flows were compared. The performance of different model outputs in HBV respectively for Neckar and Horb is shown below in Tables 6a and 6b. Likewise, the hydrographs from the best models are shown below in Figs. 10a-10d.

https://doi.org/10.5194/hess-2021-310
Preprint. Discussion started: 11 June 2021
© Author(s) 2021. CC BY 4.0 License.

Hydrology and Earth System Sciences
Discussions

Similarly, this validation was also done in Reuss catchment in Switzerland. The results are shown below in Table 7 and Figs.11a and 11b. The results and the hydrograph plots show increased overall as well as winter performance in terms of NSE in almost all the catchments. The improvement in NSEs, albeit less, is notable. This can be further explained by the reduction in mean squared errors by 15% in Reuss, 11.5% in Neckar and 3.8% in Horb. It can be thus be argued that the snow-distribution calibrated models can bolster the hydrological model outputs with an added reliability of snow-distribution.

Table 6. Performance evaluation of the snow-model outputs in HBV

(a) Neckar in Baden-Wuerttemberg

Models	**Overall NSE**	**NSE, winter**	**NSE, Snow days**	**Model description**
Basic HBV	0.871	0.858	0.841	HBV with snow component
Liq HBV + Model 1	0.869	0.853	0.834	Standard DDF melt
Liq HBV + Model 2	0.876	0.867	0.853	Model 1 + precipitation induced melt
Liq HBV + Model 3	0.867	0.854	0.834	Model 2 + sftmp + smtmp
Liq HBV + Model 4	0.868	0.855	0.825	Model 2 + smtmp + distributed sftmp
Liq HBV + Model 5	**0.885**	**0.881**	**0.872**	Model 2 + sftmp + distributed smtmp
Liq HBV + Model 6	0.871	0.86	0.841	Model 3 + Radiation induced melt
Liq HBV + Model 6.1	0.874	0.864	0.848	Model 5 + Radiation induced melt

(b) Horb in Baden-Wuerttemberg

Models	**Overall NSE**	**NSE, winter**	**NSE, Snow days**	**Model description**
Basic HBV	0.841	0.844	0.807	HBV with snow component
Liq HBV + Model 1	0.793	0.779	0.7	Standard DDF melt
Liq HBV + Model 2	0.834	0.835	0.788	Model 1 + precipitation induced melt
Liq HBV + Model 3	0.846	0.85	0.811	Model 2 + sftmp + smtmp
Liq HBV + Model 4	0.845	0.848	0.809	Model 2 + smtmp + distributed sftmp
Liq HBV + Model 5	0.846	0.85	0.811	Model 2 + sftmp + distributed smtmp
Liq HBV + Model 6	**0.847**	**0.851**	**0.813**	Model 3 + Radiation induced melt

10 Discussion

It is a big challenge and a highly imperative one, to improve the snow-melt routines in widely and successfully tested rainfall-runoff models like HBV (Bergström, 2006; Girons Lopez et al., 2020). With this backdrop, this study implemented a unique image-based pattern calibration approach using MODIS-inferred snow-distribution for a certain cloud-free day and for a duration of snow season of a given year. The MODIS data available freely across the world and at a daily resolution, provides a

https://doi.org/10.5194/hess-2021-310
Preprint. Discussion started: 11 June 2021
© Author(s) 2021. CC BY 4.0 License.

Hydrology and Earth System Sciences
Discussions
Open Access
EGU

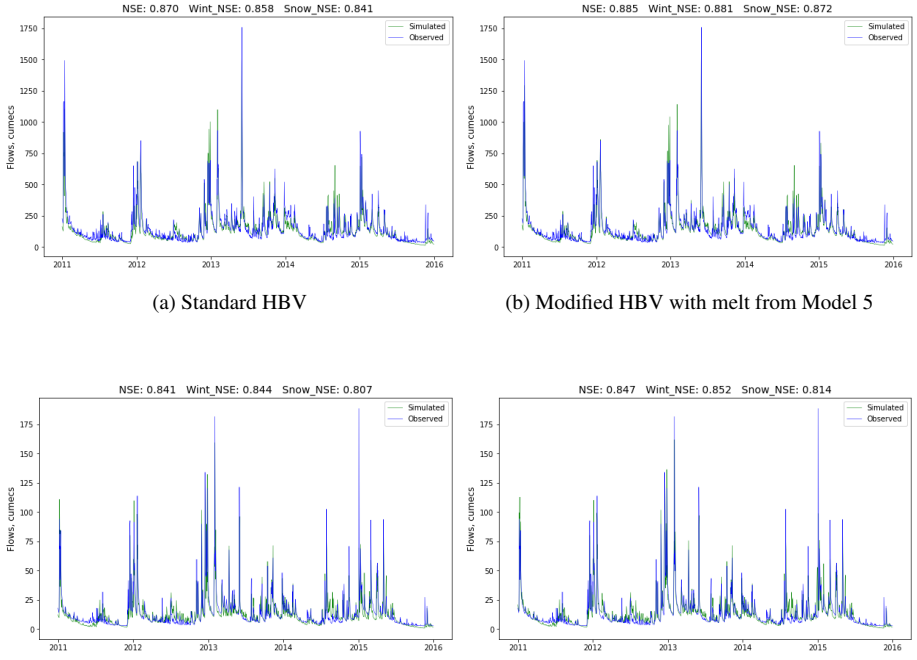

(a) Standard HBV (b) Modified HBV with melt from Model 5

(c) Standard HBV (d) Modified HBV with melt from Model 6

Figure 10. Simulated and observed hydrographs with NSE performance in Neckar in Baden-Wuerttemberg (upper row: Neckar catchment, lower row: Horb catchment)

Table 7. Performance evaluation of the snow-model outputs in HBV for Reuss catchment in Switzerland

Models	**Overall NSE**	**NSE, winter**	**NSE, Snow days**	**Model description**
Basic HBV	0.859	0.833	0.859	HBV with snow component
Liq HBV + Model 1	0.861	0.834	0.861	Standard DDF melt
Liq HBV + Model 2	0.865	0.841	0.865	Model 1 + precipitation induced melt
Liq HBV + Model 3	0.876	0.856	0.876	Model 2 + sftmp + smtmp
Liq HBV + Model 4	0.87	0.848	0.87	Model 2 + smtmp + distributed sftmp
Liq HBV + Model 5	**0.878**	**0.858**	**0.878**	Model 2 + sftmp + distributed smtmp
Liq HBV + Model 6	**0.873**	**0.853**	**0.88**	Model 3 + Radiation induced melt

plausible alternative to ground based data for immediate verification of snow-melt models. Widely used and computationally simplistic temperature index models with low data requirement were considered in the study and were modified wherever possible, to gain enhanced model performance. The Residual Kriging incorporating X,Y coordinates and directionally smoothed DEMs showed very good agreement in Switzerland and Baden-Wuerttemberg regions during the leave-one-out cross validation with NSEs for the winter season (October – April) ranging from 0.56 to 0.97. The NSE performance of the Kriging decreased

https://doi.org/10.5194/hess-2021-310
Preprint. Discussion started: 11 June 2021
© Author(s) 2021. CC BY 4.0 License.

Hydrology and Earth System Sciences
Discussions
Open Access
EGU

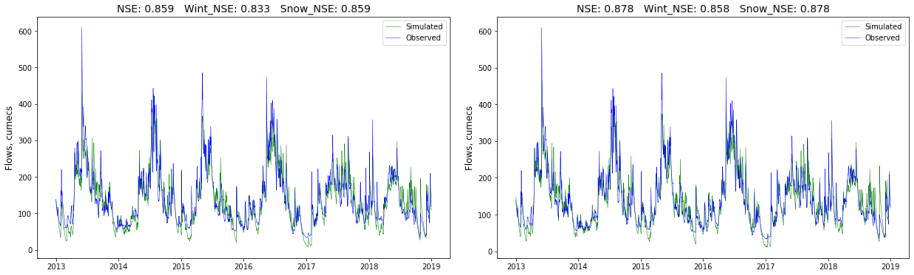

(a) Standard HBV (b) Modified HBV with melt from Model 5

Figure 11. Simulated and observed hydrographs with NSE performance in Reuss catchment, Switzerland

with increasing elevation in Switzerland. No clear pattern as such was observed in Baden-Wuerttemberg. For temperature, the External Drift Kriging was also able to simulate the observed values in both regions. We further found out that all the model variants were able to track the MODIS snow-distribution with higher accuracy. However, the melt-model with the daily potential clear-sky radiation was able to perform the best among the considered model variants. The model was able to simulate the snow cover distribution with a higher accuracy to identify snow and no-snow pixels, reflected on the lower Brier-score values. The calibrated model was also able to track the evolution and depletion of snow adeptly throughout the snow seasons in different years. The inclusion of radiation induced melt provides a more realistic spatial distribution of melt rates (Hock, 1999). The model parameters were then tested for temporal stability across different seasons and years. The hindcasting, calibration and forecasting results show that model parameters calibrated for each season are more or less stable without much fluctuations, in Switzerland. This was, however, slightly different in Baden-Wuerttemberg as the calibrated parameters for different years depicted higher scatter. This could be due to lesser and more uncertain snow-availability in comparison to Switzerland. It is noteworthy that the parameters identified as optimum for the Swiss region also perform well as compared to the calibrated Brier scores in all the calibration periods. This bolsters the objective of this study to obtain spatio-temporal robustness of the model parameters. We found out that with continuous model updating, the MODIS data can be used to guide the snow-melt forecast in the regions with snow-melt as primary water source. Finally, the melt outputs from the best models were selected as standalone inputs to a modified HBV model and the resulting hydrographs for Reuss in Switzerland and, Neckar and Horb in Baden-Wuerttemberg were assessed. The results suggested that these modified HBV models had slightly better NSE performance than the calibrated HBV models for the catchments in the region. However, 3.8-15% decrease in mean squared errors were observed for all the catchments under study. The not-so significant gain in NSE performance can be attributed to HBV's simplistic generalization of the real processes and the behaviour outputs at the chosen spatio-temporal resolution (Girons Lopez et al., 2020; Magnusson et al., 2014) . Nevertheless, we were able to infer that the improvement in NSEs, albeit less, can be achieved with an added reliability of snow-distribution.

https://doi.org/10.5194/hess-2021-310
Preprint. Discussion started: 11 June 2021
© Author(s) 2021. CC BY 4.0 License.

Hydrology and Earth System Sciences
Discussions

11 Conclusions

We assessed the potential of freely available snow cover distribution from daily resolution MODIS data to calibrate the snow-melt models on snow-pattern instead of a more traditional SWE and flow based calibration in the snow-dominated regimes in Switzerland and Baden-Wuerttemberg region in Germany. Specifically, different model modifications were employed to assess the improvement in the simulation of snow-distribution with lesser input requirements. It was observed that the methodology does well in reproducing the snow cover distribution in the regions with relative higher accuracy. The results differ in terms of snow-availability with Switzerland showing better results than Baden-Wuerttemberg which is characterized by less snow. The model incorporated with radiation induced melt showed more promise and was selected for further analysis in the study. The parameters depict good temporal stability and with continuous updating provide a potential for forecasting snow-availability in the regions. The application of the melt-model outputs in HBV increased the NSE performance to some extent and in conjunction with this approach, simpler specific alterations to processes contributing to snow-melt can contribute to identifying the snow-distribution and to some extent the flows in snow-dominated regimes. We can conclude that calibration using readily available images used in this method offers adequate flexibility, albeit the simplicity, to calibrate snow distribution in mountainous areas across a wide geographical extent with reasonably accurate precipitation and temperature data. This also adds value to provide improved conceptualization of the temperature-index model routines and further potential model updating.

Data availability. The precipitation and temperature data were obtained from the Climate Data Center of the German Weather Service (DWD; https://opendata.dwd.de/climate_environment/CDC, last access: 15 February 2021) (DWD, 2021) and the Swiss Federal Office of Meteorology and Clima-tology (MeteoSwiss; https://gate.meteoswiss.ch/idaweb, last access: 21 Decemeber, 2020)(MeteoSwiss, 2020). The MODIS snow cover images were downloaded using the Earth Data Search tool (https://search.earthdata.nasa.gov, last access: 19 Feb 2021)

Author contributions. This study is a part of DG's doctoral research supervised by AB. The study was conceptualized by AB and DG, and was implemented by DG. Both authors contributed to the writing, reviewing and editing of the paper.

Competing interests. The authors declare that they have no conflict of interest.

Acknowledgements. The authors would like to acknowledge Deutscher Akademischer Austauschdienst (DAAD) for the doctoral research scholarship which encompasses this study.

Financial support. This open-access publication was funded by the University of Stuttgart.

https://doi.org/10.5194/hess-2021-310
Preprint. Discussion started: 11 June 2021
© Author(s) 2021. CC BY 4.0 License.

Hydrology and Earth System Sciences
Discussions

References

Bańdossy, A. and Pegram, G.: Interpolation of precipitation under topographic influence at different time scales, Water Resources Research, 49, 4545–4565, https://doi.org/https://doi.org/10.1002/wrcr.20307, 2013.

Bergström, S.: Experience from applications of the HBV hydrological model from the perspective of prediction in ungauged basins, IAHS-AISH publication, pp. 97–107, 2006.

Bergström, S.: The HBV model., chap. Computer models of watershed hydrology, pp. 443–476, Water Resources Publications, Colorado, USA, 1995.

Feng, X., Sahoo, A., Arsenault, K., Houser, P., Luo, Y., and Troy, T. J.: The Impact of Snow Model Complexity at Three CLPX Sites, Journal of Hydrometeorology, 9, 1464–1481, https://doi.org/10.1175/2008JHM860.1, 2008.

Gafurov, A. and Bárdossy, A.: Cloud removal methodology from MODIS snow cover product, Hydrology and Earth System Sciences, 13, 1361–1373, https://doi.org/10.5194/hess-13-1361-2009, 2009.

Girons Lopez, M., Vis, M. J. P., Jenicek, M., Griessinger, N., and Seibert, J.: Assessing the degree of detail of temperature-based snow routines for runoff modelling in mountainous areas in central Europe, Hydrology and Earth System Sciences, 24, 4441–4461, https://doi.org/10.5194/hess-24-4441-2020, 2020.

Hall, D., Salomonson, V., and Riggs, G.: MODIS/Terra Snow Cover 5-Min L2 Swath 500m, Version 5. Boulder, Colorado USA., NASA National Snow and Ice Data Center Distributed Active Archive Center, https://doi.org/10.5067/ACYTYZB9BEOS, 2006.

He, Z. H., Parajka, J., Tian, F. Q., and Blöschl, G.: Estimating degree-day factors from MODIS for snowmelt runoff modeling, Hydrology and Earth System Sciences, 18, 4773–4789, https://doi.org/10.5194/hess-18-4773-2014, 2014.

Hock, R.: A distributed temperature-index ice- and snowmelt model including potential direct solar radiation, Journal of Glaciology, 45, 101–111, https://doi.org/10.3189/S0022143000003087, 1999.

Hock, R.: Temperature index melt modelling in mountain areas, Journal of Hydrology, 282, 104–115, https://doi.org/https://doi.org/10.1016/S0022-1694(03)00257-9, mountain Hydrology and Water Resources, 2003.

Hofierka, J. and Suri, M.: The solar radiation model for Open source GIS: implementation and applications, Proceedings of the Open source GIS - GRASS users conference 2002, 2002.

Kirkham, J. D., Koch, I., Saloranta, T. M., Litt, M., Stigter, E. E., Møen, K., Thapa, A., Melvold, K., and Immerzeel, W. W.: Near Real-Time Measurement of Snow Water Equivalent in the Nepal Himalayas, Frontiers in Earth Science, 7, 177, https://doi.org/10.3389/feart.2019.00177, 2019.

Magnusson, J., Gustafsson, D., Hüsler, F., and Jonas, T.: Assimilation of point SWE data into a distributed snow cover model comparing two contrasting methods, Water Resources Research, 50, 7816–7835, https://doi.org/https://doi.org/10.1002/2014WR015302, 2014.

Neteler, M. and Mitasova, H.: Open source GIS: a GRASS GIS approach - Appendix, vol. 689, Kluwer Academic Pub, 2002.

Parajka, J. and Blöschl, G.: The value of MODIS snow cover data in validating and calibrating conceptual hydrologic models, Journal of Hydrology, 358, 240–258, https://doi.org/https://doi.org/10.1016/j.jhydrol.2008.06.006, 2008.

Rutter, N., Essery, R., Pomeroy, J., Altimir, N., Andreadis, K., Baker, I., Barr, A., Bartlett, P., Boone, A., Deng, H., Douville, H., Dutra, E., Elder, K., Ellis, C., Feng, X., Gelfan, A., Goodbody, A., Gusev, Y., Gustafsson, D., Hellström, R., Hirabayashi, Y., Hirota, T., Jonas, T., Koren, V., Kuragina, A., Lettenmaier, D., Li, W., Luce, C., Martin, E., Nasonova, O., Pumpanen, J., Pyles, R., Samuelsson, P., Sandells, M., Schädler, G., Shmakin, A., Smirnova, T., Stähli, M., Stöckli, R., Strasser, U., Su, H., Suzuki, K., Takata, K., Tanaka, K., Thompson,

https://doi.org/10.5194/hess-2021-310
Preprint. Discussion started: 11 June 2021
© Author(s) 2021. CC BY 4.0 License.

Hydrology and Earth System Sciences
Discussions
Open Access
EGU

E., Vesala, T., Viterbo, P., Wiltshire, A., Xia, K., Xue, Y., and Yamazaki, T.: Evaluation of forest snow processes models (SnowMIP2), Journal of Geophysical Research, https://doi.org/10.1029/2008JD011063, 12.01.03; LK 01; 114(D06111), 2009, 2009.

Schmucki, E., Marty, C., Fierz, C., and Lehning, M.: Evaluation of modelled snow depth and snow water equivalent at three contrasting sites in Switzerland using SNOWPACK simulations driven by different meteorological data input, Cold Regions Science and Technology, 99, 27–37, https://doi.org/https://doi.org/10.1016/j.coldregions.2013.12.004, 2014.

Tran, H., Nguyen, P., Ombadi, M., lin Hsu, K., Sorooshian, S., and Qing, X.: A cloud-free MODIS snow cover dataset for the contiguous United States from 2000 to 2017, Sci Data, 6, https://doi.org/10.1038/sdata.2018.300, 2019.

Wang, X. and Xie, H.: New methods for studying the spatiotemporal variation of snow cover based on combination products of MODIS Terra and Aqua, Journal of Hydrology, 371, 192–200, https://doi.org/https://doi.org/10.1016/j.jhydrol.2009.03.028, 2009.